Cell Stress and Chaperones (2017) 22:43–54
DOI 10.1007/s12192-016-0740-2

ORIGINAL PAPER

Moderate endoplasmic reticulum stress activates a PERK and p38-dependent apoptosis

Emily C. Lumley[1] · Acadia R. Osborn[1] · Jessica E. Scott[1] · Amanda G. Scholl[1] · Vicki Mercado[1] · Young T. McMahan[1] · Zachary G. Coffman[1] · Jay L. Brewster[1]

Received: 17 May 2016 / Revised: 5 October 2016 / Accepted: 7 October 2016 / Published online: 20 October 2016

Abstract The endoplasmic reticulum (ER) has the ability to signal organelle dysfunction via a complex signaling network known as the unfolded protein response (UPR). In this work, hamster fibroblast cells exhibiting moderate levels of ER stress were compared to those exhibiting severe ER stress. Inhibition of N-linked glycosylation was accomplished via a temperature-sensitive mutation in the Dad1 subunit of the oligosaccharyltransferase (OST) complex or by direct inhibition with tunicamycin (Tm). Temperature shift (TS) treatment generated weak activation of ER stress signaling when compared to doses of Tm that are typically used in ER stress studies (500–1000 nM). A dose-response analysis of key ER stress signaling mediators, inositol-requiring enzyme 1 (IRE1) and protein kinase R (PKR)-like endoplasmic reticulum kinase (PERK), revealed 20–40 nM of Tm to generate activation intensity similar to TS treatment. In parental BHK21 cells, moderate (20–40 nM) and high doses (200–1000 nM) of Tm were compared to identify physiological and signaling-based differences in stress response. Inhibition of ER Ca^{2+} release via ITPR activity with 2-aminoethoxydiphenyl borate (2-APB) or Xestospongin C (XeC) was sufficient to protect against apoptosis induced by moderate but not higher doses of Tm. Analysis of kinase activation over a range of Tm exposures revealed the p38 stress-activated protein kinase (SAPK) to display increasing activation with Tm dosage. Interestingly, Tm induced the extracellular regulated kinases (Erk1/2) only at moderate doses of Tm. Inhibition of ER transmembrane stress sensors (IRE1, PERK) or cytosolic signaling mediators (p38, Jnk1, Erk1/2) was used to evaluate pathways involved in apoptosis activation during ER stress. Inhibition of either PERK or p38 was sufficient to reduce cell death and apoptosis induced by moderate, but not high, doses of Tm. During ER stress, cells exhibited a rapid decline in anti-apoptotic Mcl-1 and survivin proteins. Inhibition of PERK was sufficient to block this affect. This work reveals moderate doses of ER stress to generate patterns of stress signaling that are distinct from higher doses and that apoptosis activation at moderate levels of stress are dependent upon PERK and p38 signaling. Studies exploring ER stress signaling should recognize that this signaling acts as a rheostat rather than a simple switch, behaving distinctively in a dose-dependent manner.

Keywords Endoplasmic reticulum · Protein folding · Apoptosis · p38 kinase · Protein kinase R (PKR)-like endoplasmic reticulum kinase · PERK · Unfolded protein response

Abbreviations

ER	Endoplasmic reticulum
Tm	Tunicamycin
TS	Temperature shift
2-APB	2-Aminoethoxyphenylborate
OST	Oligosaccharyltransferase
XeC	Xestospongin C
IRE1	Inositol-requiring enzyme 1
PERK	Protein kinase R (PKR)-like endoplasmic reticulum kinase
Xbp1	X-box binding protein 1
ITPR	Inositol 1,4,5-trisphosphate receptor
RT/PCR	Reverse transcription, polymerase chain reaction
UPR	Unfolded protein response

✉ Jay L. Brewster
jay.brewster@pepperdine.edu

[1] Natural Science Division, Pepperdine University, 24255 Pacific Coast Highway, Malibu,, CA 90263, USA

Introduction

The endoplasmic reticulum (ER) is responsible for approximately 50 % of cellular protein synthesis and the bulk of lipid biosynthetic processes. The generation of a functional protein product involves the complex process of establishing the native state of conformation and then exporting that protein from the ER via the secretory pathway. Protein folding to achieve the native state involves chaperone-mediated folding, formation of disulfide bonds, and glycosylation additions at appropriate asparagine (N-linked) and serine/threonine (O-linked) sites. Quality control assessments of each protein are made through associations with chaperones in the calnexin/calreticulin cycle, facilitating export of properly folded proteins, reprocessing of misfolded proteins, or destruction of proteins that repeatedly fail quality control assessments. Even during normal cellular conditions, there are significant numbers of proteins that are rejected during ER assessments and are retrotranslocated to the cytosol for proteolytic destruction by the proteasome (Ruggiano et al. 2014). Accumulation of misfolded proteins within the ER can overwhelm the quality control program, resulting in activation of stress signaling to induce heightened expression of chaperone and other processing proteins, a signaling network known as the unfolded protein response (UPR).

Stress signaling from the ER is complex, generating adaptive cellular responses to restore normal functional capacity of the ER and apoptotic signaling in response to sustained ER stress (Walter and Ron 2011; Hetz 2012). The UPR is primarily signaled through three signal initiators localized to the ER membrane: the inositol-requiring enzyme 1 (IRE1), the eIF2α kinase 3 (EIF2AK3 or PERK), and activating transcription factor 6 (ATF6) (Lee 2005). Active IRE1 oligomers display trans-autophosphorylation and endoribonuclease activity. The IRE1 endoribonuclease activity influences cellular gene expression through two processes: (1) the splicing of a 26-nucleotide intron from the X-box binding protein 1 (*Xbp1*) pre-messenger RNA (mRNA), enabling translation of this UPR transcription factor (Walter and Ron 2011; Schroder 2008), and (2) by degrading select mRNAs and small RNAs through cleavage, known as the regulated IRE1-dependant degradation of mRNA (RIDD) (Maurel et al. 2014). The PERK transmembrane protein also oligomerizes and displays trans-autophosphorylation when activated from the ER lumen. The central substrate for PERK kinase activity is the cytosolic eIF2α translational initiation factor. Phosphorylation of eIF2α results in an arrest of general cellular translation and an activation of translation of a rare subset of mRNAs that includes the activating transcription factor 4 (ATF4) (Wek et al. 2006). The activation of ATF6 results in its relocalization to the Golgi apparatus and a subsequent proteolytic cleavage to release a transcriptionally active 50 kDa protein. The central UPR-initiating event in the ER lumen is a rise in inappropriately folded proteins, with exposed hydrophobic domains that can interact with luminal binding domains of stress sensors in the ER membrane (Gardner et al. 2013). In addition, the Grp78 Ca^{2+}-dependent chaperone within the ER lumen is known to regulate stress sensors. In normal conditions, the pool of available Grp78 is distributed between misfolded proteins in the ER lumen and the stress sensors themselves. An accumulation of misfolded proteins causes a redistribution of Grp78 to the lumen, releasing the ER sensors. This release is hypothesized to enable formation of oligomers, though full activation of the sensors requires association with misfolded proteins (Gardner and Walter 2011). The net result of ER stress activation is elevation of transcription factors that induce an adaptive response and an interruption of normal cellular gene expression.

Activation of apoptosis in response to ER stress is known to involve several distinct signaling pathways, ultimately leading to the mitochondrial permeability transition (mPT) and caspase activation. Sustained ER stress induces IRE1 ubiquitination and formation of an IRE1/TRAF2/JNK1 signaling complex at the cytosolic periphery of the ER (Zhu et al. 2014). The RIDD activity of IRE1 is known to de-repress expression of caspase 2, increasing levels of apoptosis (Hassler et al. 2012; Upton et al. 2012). PERK phosphorylation of the eIF2a translation initiation factor results in arrest of most cellular translation but simultaneously increases production of ATF4, whose activity increases expression of pro-apoptotic genes such as Gadd153/CHOP (Hiramatsu et al. 2015). Other stress signaling from the ER includes the release of Ca^{2+} from ER stores via the inositol 1,4,5-trisphosphate receptor (ITPR) (Higo et al. 2010; Boehning et al. 2003; Blackshaw et al. 2000; Joseph and Hajnoczky 2007) and a physical interaction with ER-embedded mitochondria that plays a role in apoptosis activation (Hoppins and Nunnari 2012). Apoptotic signaling from the ER has been a dynamic area of research, with several known downstream signal mediators. Results to this point have identified varied dynamics depending upon stressor, context, and cell type.

Derived from BHK21 hamster kidney cells, the tsBN7 cell line carries a substitution mutation within Dad1, an essential subunit of the ER membrane-localized oligosaccharyltransferase (OST) complex responsible for N-linked glycosylation of nascent proteins synthesized at the ER (Sanjay et al. 1998; Nakashima et al. 1993; Brewster et al. 2000). This mutation generates a temperature-sensitive N-linked glycosylation activity; cells are phenotypically normal at 32.5 °C, but at 39.5 °C display a dramatic decrease in N-linked glycosylation, activation of ER stress signaling, and intrinsic apoptosis (Niederer et al. 2005). When exposed to chemical activators of ER stress, tsBN7 and BHK21 cells display similar patterns of stress signaling, with induction of Grp78 and CHOP expression, and a similar pattern of cell death activation. However, pharmacological inhibition of N-linked glycosylation with tunicamycin (Tm)

generates apoptotic signaling that is distinct from temperature shift (TS) treatment (Niederer et al. 2005). In particular, TS-treated cells can be rescued from ER stress-induced apoptosis with cyclosporine A or type II pyrethroids. As both signals originate with a defect in protein glycosylation, the differences in signaling behavior are interesting. Analysis of N-linked glycosylation in tsBN7 cells and DAD1$^{-/-}$ embryonic fibroblasts revealed the loss of the Dad1 from the OST complex diminishes severely but does not completely ablate N-linked glycosylation (Hong et al. 2000; Nikonov et al. 2002). Thus, the difference between TS-treated and Tm-treated tsBN7 cells is likely due to severity of glycosylation defect. We hypothesized that ER stress signaling responses are sensitive to the severity of defect and that stress severity may impact the array of signals used to activate apoptosis. In this work, we have sought to examine the basis of these differences more carefully and to evaluate cellular behavior responding to ER stress of varied severity.

Methods and materials

Cell culture

Dulbecco's modified Eagle's medium (DMEM), antibiotic/antimycotic (penicillin/streptomycin/amphotericin B), fetal bovine serum, non-essential amino acids, and trypsin were manufactured by Gibco BRL (ThermoFisher Scientific, Waltham, MA). BHK21 hamster fibroblast cells were purchased from the American Tissue Culture Collection (ATCC, Manassas, VA). The BHK21-derived tsBN7 cell line was provided courtesy of Dr. Claudio Basilico, NYU Medical School. BHK21 cells were cultured at 5 % CO_2 and a temperature of 37 °C. tsBN7 cells were cultured at 32.5 °C and shifted to 39.5 °C to activate the TS phenotype. Cells were passaged every 3–4 days to maintain appropriate cell density. For the purpose of controlling cell density during seeding of experiments, cells in suspension were assayed for density by using a Scepter cell counter (EMD Millipore, San Diego, CA).

Media additives, antibodies, and immunoblotting

Tunicamycin, salubrinal, and 2-aminoethoxydiphenylborate (2-APB) were purchased from Sigma (St. Louis, MO). Cell-permeable inhibitors of signaling proteins, ERK inhibitor II, p38 inhibitor III, IRE1 inhibitor 4u8c, IRE1 kinase inhibitor KIRA6, PERK inhibitor I, and JNK inhibitor VIII (420135) were purchased from Calbiochem (EMD Millipore, San Diego, CA). Antibodies were purchased from Cell Signaling Technologies (Madison, WI) unless noted otherwise. Mcl-1 antibodies were purchased from Rockland Immunochemicals (Pottstown, PA). Xestospongin C (ITPR inhibitor) and the CHOP antibody were purchased from Santa Cruz Biotechnology (Santa Cruz, CA). Antibodies against tubulin were purchased from the Developmental Studies Hybridoma Bank at the University of Iowa (Iowa City, IA).

Immunoblots were performed according to established protocols. Adherent cells were rapidly lysed in a heated (95 °C) solution of 2 % SDS, 62.5 mM Tris-HCl (pH 6.8), and 7 % glycerol. Triturated samples were assayed for protein concentration by using the bicinchoninic acid assay (BCA assay kit; ThermoFisher Scientific). Protein gels were transferred to PVDF-FL (EMD Millipore, San Diego, CA), blocked, and probed with the appropriate antibody combination. Detection of antibody binding was accomplished with infrared dye-conjugated secondary antibodies (IRDye) and infrared scanning at 680 or 800 nm. Infrared-conjugated dyes and the Odyssey infrared scanner are products of LI-COR (Lincoln, NE).

Cell imaging and density detection

Cell survival assays were performed as previously described (Niederer et al. 2005). Seeding density for cell survival assays was 15,000 cells/cm^2, with a 30-h recovery period prior to experimental treatment. Cells were treated as described, and the following treatments were fixed in 4 % paraformaldehyde for 20 min, washed with PBS, and stained with a 0.3 % crystal violet dye solution for an additional 20 min. Plates were washed with water and then dried before scanning absorbance at 590 nm. Assessments of apoptotic nuclei were performed in a similar manner, with fixed cells being washed, but then mounted under a coverslip in ProLong Gold antifade mountant with DAPI (ThermoFisher Scientific). Cells were scored as apoptotic if they displayed condensed and/or fragmented nuclear morphology. For statistical analysis of data generated from counting of nuclear morphology, percentages were modified via angular transformation (arcsin square root transformation) prior to statistical analysis. Immunocytochemistry analysis for caspase-3 activation was performed on cells cultured on treated glass slides. Fixed cells were permeabilized for 1 h at 4 °C (1× DPBS, 5 % BSA, 0.2 % Triton X-100, 0.1 % sodium azide), antibody exposed for 12 h at 4 °C (identical solution with the exception of 2 % BSA), washed in cold DPBS, exposed to fluorescently labeled secondary antibody in DPBS at room temperature, washed, and mounted in antifade as described above.

Quantification of Xbp1 RNA splicing

The ER-localized IRE1 transmembrane protein splices Xbp1 RNA in response to stress within the ER lumen. Quantification of Xbp1 RNA splicing is an accessible measure of ER stress severity. Total RNA was purified from cells by using the RNeasy Mini Kit (Qiagen, Chatsworth, CA) followed by complementary DNA (cDNA) synthesis and polymerase chain reaction amplification (RT-PCR). The cDNA synthesis was performed with MessageSensor RT Kit protocol (Ambion Inc.,

Austin, TX), and PCR was performed with *Taq* DNA polymerase (New England BioLabs, Ipswich, MA). PCR primers for Xbp1 cDNAs were (forward) 5′-CACCTGAGCCCCGAGGAG-3′ and (reverse) 5′-TTAGTTCATTAATGGCTTCCAGC-3′ which span a 26 bp intron (Sigma-Aldrich, The Woodlands, TX). These primers amplify a 599 bp product containing the intron and a 573 bp product following splicing of Xbp1 to a functional mRNA. PCR products were run on a 3 % agarose gel and ethidium bromide-labeled DNA quantified by using ultraviolet light and digital image capture.

Cell fractionation

Analysis of protein distribution among membrane (mitochondria/ER) and cytosolic cellular compartments was performed by cell fractionation and western blot analysis. Cell fractionation was performed by using the Qiagen Qproteome Cell Compartment and Fractionation Kit (Qiagen, Santa Clarita, CA). Cultured cells were trypsinized, chilled to 4 °C, and lysed to release cytosolic contents while maintaining organelle and nuclear integrity. Subsequent fractions were generated for the membrane, nuclear and cytoskeletal proteins. Fractions were assayed for protein concentration and analyzed by SDS-PAGE according to established protocols.

Results

Genetic defect in N-linked glycosylation activates a distinct ER stress signal

A comparison of phenotype induced by deficient N-linked glycosylation was examined in BHK21-derived tsBN7 cells. Stress signaling induced by Tm treatment or TS (39.5 °C) was initially assessed with two known inhibitors of ER stress-induced apoptosis. Both Tm and TS-treated tsBN7 cells activate a clear apoptotic response, with elevated expression of UPR genes, stress-activated protein kinase (SAPK) activation, and activation of the mitochondrial permeability transition (Niederer et al. 2005). Salubrinal inhibits phosphatase activity responsible for dephosphorylating/reactivating eIF2a during a period of ER stress, and this inhibition has been shown to be protective if used at acute timepoints (Boyce et al. 2005; Kessel 2006; Cnop et al. 2007; Wu et al. 2014). Release of ER Ca^{2+} via ITPR activity can be specifically inhibited with appropriate doses of 2-APB or Xestospongin C (XeC) (Ascher-Landsberg et al. 1999; Saleem et al. 2014; Miyamoto et al. 2000). In TS-treated cells, but not Tm-treated cells, salubrinal or 2-APB treatment reduces the levels of stress-induced Grp87 or CHOP expression and caspase 3 activation (Fig. 1a, b). A 36-h exposure of tsBN7 cells to either TS or Tm (1 μM) generated apoptotic nuclear morphology in approximately 35 % of evaluated cells (Fig. 1c). When 2-APB was included with the TS treatment, cells were significantly protected from ER stress-induced apoptotic activation. In Tm-treated cells, 2-APB provided no protection from ER stress-induced death. To evaluate if the TS treatment was conferring any kind of protection due to heat shock-induced factors, BHK21 cells were also evaluated. Tunicamycin treatment of the parental BHK21 cells displayed a similar activation of apoptosis at both 37 °C and under TS treatment conditions. These results reveal a clear phenotypic distinction between the TS and Tm (1 μM) conditions in tsBN7 cells. This distinction in signal susceptibility to inhibition was surprising, and subsequent experiments examined the hypothesis that this distinction was due to differences in the intensity or character of the ER stress exhibited under each condition.

Key quantitative measures of ER stress signaling intensity are IRE1-mediated splicing of *Xbp1* RNA and PERK phosphorylation of eIF2α. To assess IRE1 activation, spliced and non-spliced *Xbp1* RNAs are quantitatively assessed by using reverse transcription followed by PCR amplification across the intron/splice site. An initial assessment of the timing of *Xbp1* splicing during TS and Tm (1 μM) exposure revealed a transient peak of splicing activity that appears between 6 and 12 h post treatment (Fig. 2a). Peak splicing activity for Tm-treated (1 μM) cells was typically measured at 70–80 % spliced, while TS-treated cells displayed a typical peak at 35–45 % spliced. Evaluation of splicing activity over a range of Tm concentrations revealed a clear dose-response relationship, with splicing activity displaying a plateau beginning at approximately 200 nM (Fig. 2b). tsBN7 cells exposed to TS conditions displayed a level of splicing that correlates with Tm exposures at approximately 20–40 nM. To evaluate kinase activity exhibited by the PERK ER sensor, eIF2α phosphorylation was similarly evaluated over a time course of TS conditions. Significant increases in eIF2α phosphorylation were observed 6–12 h post TS exposure, which then subsided within 36 h (Fig. 2c). Maximal TS-induced eIF2α phosphorylation increases (1.36-fold, 6 h) were similar to levels generated by 30 nM Tm exposure for 6 h (Fig. 2d). IRE1 has the capacity to induce JNK (SAPK) activity during ER stress via phosphorylation of this cytosolic kinase. Neither TS nor Tm conditions activated clear phosphorylation of JNK in these cells (Fig. 2c/d). In summary, these analyses reveal TS-induced stress in tsBN7 cells to activate IRE1 splicing activity and PERK kinase activity at levels approximating a moderate dosage of Tm (20–40 nM). This concentration of Tm is 25-fold below concentrations typically used to activate ER stress in cell culture experiments.

ITPR inhibition protects BHK21 cells from moderate ER stress

Analysis of *Xbp1* pre-mRNA splicing in tsBN7 cells indicated Tm doses between 20 and 40 nM created ER stress signaling

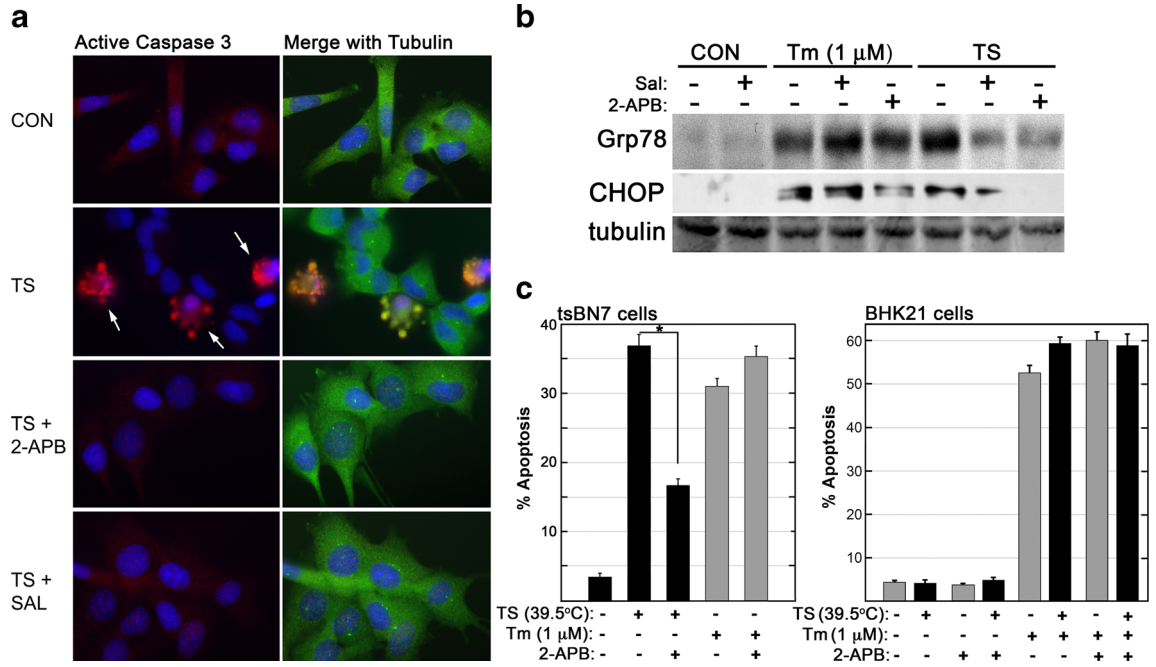

Fig. 1 Distinct apoptotic responses by cells experiencing deficient N-linked glycosylation. **a** tsBN7 cells exposed to TS (39.5 °C, 36 h) exhibit activation of apoptosis as shown by detection of active caspase-3 via immunocytochemistry. Cells were evaluated with rabbit anti-active caspase-3 and mouse anti-tubulin. Levels of apoptosis were diminished with the addition of known inhibitors of ER stress signaling: 2-APB (50 μM) or salubrinal (10 μM). **b** Immunoblot of proteins isolated from tsBN7 cells treated with TS or tunicamycin (Tm, 1 μM) for 24 h. Inhibitors of ER stress signaling were sufficient to block TS-induced increases in expression of UPR target Grp78 and CHOP. Immunoblot data is representative of at least three independently replicated experiments. **c** tsBN7 and BHK21 cells were exposed to TS or Tm (1 μM) for 36 h and then fixed. Nuclei were stained with DAPI, mounted, and scored for percentage of cells exhibiting apoptotic nuclear morphology. In tsBN7 cells, TS but not Tm exhibited an apoptotic signal that could be inhibited by ITPR inhibition with 2-APB (50 μM). BHK21 cells treated with Tm (1 μM) displayed apoptosis induction regardless of the presence/absence of 2-APB. Statistical analysis was via Student's *t* test ($p < 0.05$)

at magnitude similar to the TS-induced phenotype. To better characterize this moderate dosage of stress in wild-type cells, the parental BHK21 hamster fibroblast cells were evaluated. Cells were treated with a range of Tm concentrations in the presence or absence of ITPR inhibitors; after incubation for 48 h, the samples were analyzed for cell density (Fig. 3a, b). ITPR inhibition was sufficient to significantly diminish Tm-induced decreases in cell density at Tm doses of 20 and 30 nM, but not at doses of 50 nM or higher. Similarly, analysis of apoptotic nuclei revealed ITPR inhibition to be significantly protective at these moderate doses of Tm (Fig. 3c), which is consistent with the TS-induced behavior observed in tsBN7 cells. In tsBN7 cells, TS-induced UPR signaling was shown to be susceptible to inhibition of ITPR-based Ca^{2+} signaling from the ER (Fig. 1b). Parental BHK21 cells were evaluated for UPR signaling in response to a low dose exposure of Tm and the presence or absence of an ITPR inhibitor. Over a time course of 36 h, 20 nM Tm was sufficient to stimulate Grp78 and Grp94 expression, which increased over time of exposure (Fig. 3d). Inclusion of 2-APB diminished Tm-stimulated increases in Grp78 and Grp94 protein levels consistent with Ca^{2+} release from the ER playing a role in signaling of the UPR during moderate stress.

Moderate and severe ER stresses generate similar levels of ER membrane porosity

Within the complex array of stress signaling that emerges from the ER, membrane integrity has been shown to play a contributing role. Two pro-apoptotic B cell lymphoma 2 (Bcl-2) family members, Bax and Bak, localize to the ER membrane during ER stress (Zong et al. 2003). Their impact upon ER signaling is complex but includes permeability of the ER membrane to release of luminal proteins (Wang et al. 2011). We hypothesized that ER membrane integrity might be differentially affected by dosage of Tm, with higher doses generating a more severe loss of membrane integrity and a pro-apoptotic release of ER components to the cytosol. In BHK21 cells expressing an ER-localized green fluorescent protein, high doses of Tm (1 μM) were shown to generate clear distortion of organelle structure and a diffuse distribution of green fluorescence (Fig. 4a). Cell fractionation experiments were used to compare ER membrane integrity during moderate and high doses of Tm exposure (20 nM and 1 μM, respectively). Both doses of Tm were sufficient to generate the cytosolic appearance of ERp57 and protein disulfide isomerase (PDI) within 24 h of stress activation (Fig. 4b). Though calreticulin is of similar size

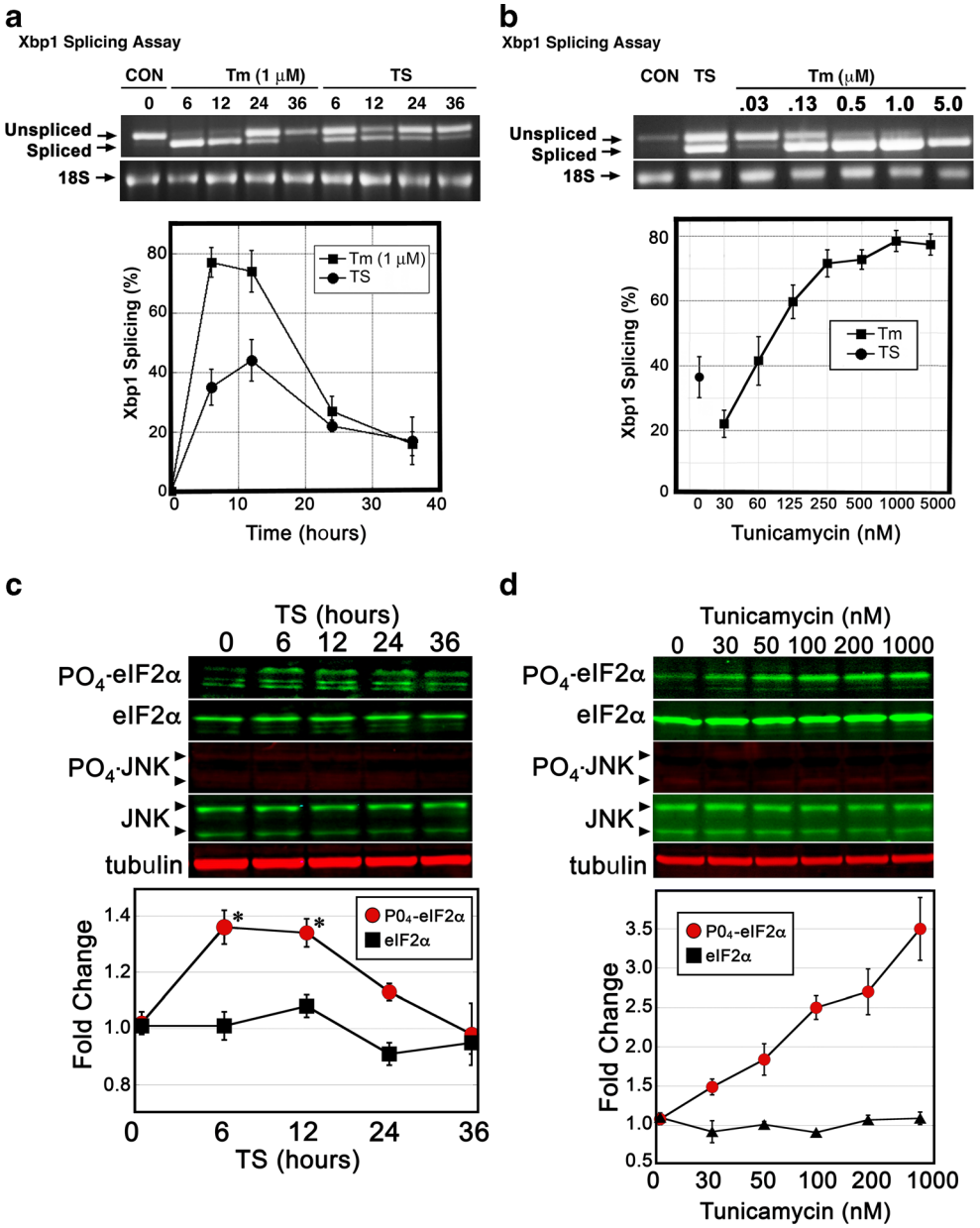

Fig. 2 The TS treatment of tsBN7 cells generates a moderate level of IRE1 and PERK activation. **a** tsBN7 cells were exposed to TS or Tm (1 μM) for the amount of time shown, lysed, and RNA purified from cell lysates. IRE1 splicing of *Xbp1* RNA was measured via RT/PCR with primers directed to opposing sides of a 26-nucleotide intron. Unspliced pre-mRNA is detected as a 599 bp *Xbp1* band, while spliced mRNA is detected as a 573 bp band. PCR products were analyzed via agarose gel electrophoresis and by digital imaging. **b** Splicing of *Xbp1* RNA was measured over a range of Tm concentrations from 30 nM to 5 μM (6-h exposure). This analysis reveals a dose-response relationship between Tm and splicing activity and that TS-treated tsBN7 cells exhibit a moderate level of splicing. **c** To assess PERK-directed phosphorylation of eIF2α, tsBN7 cells were exposed to TS conditions over 36 h. Immunoblots were performed and quantified. Attempts to detect any induced phosphorylation of JNK revealed only faint/invariant bands. **d** Analysis of eIF2α phosphorylation was measured over a range of Tm doses (6-h treatment). Phosphorylation levels rise in a dose-dependent manner, with 30 nM generating levels of eIF2a phosphorylation similar to TS. Statistical analysis of quantification of immunoblots was by ANOVA with a Tukey's all pairs post hoc test comparing treated samples at each timepoint to control ($p < 0.05$)

(55 kDa) to PDI and ERp57, no appearance in the cytosol during ER stress was identified. This assessment of ER membrane integrity confirmed that moderate and severe ER stress each affect integrity of the ER membrane but did not reveal elevated severity of the phenotype in response to Tm dosage.

Inhibition of PERK and p38 (SAPK) protects against moderate but not severe ER stress

To better characterize the nature of stress signaling from the ER over a range of Tm exposures, evaluations of Erk1/2 (p42/

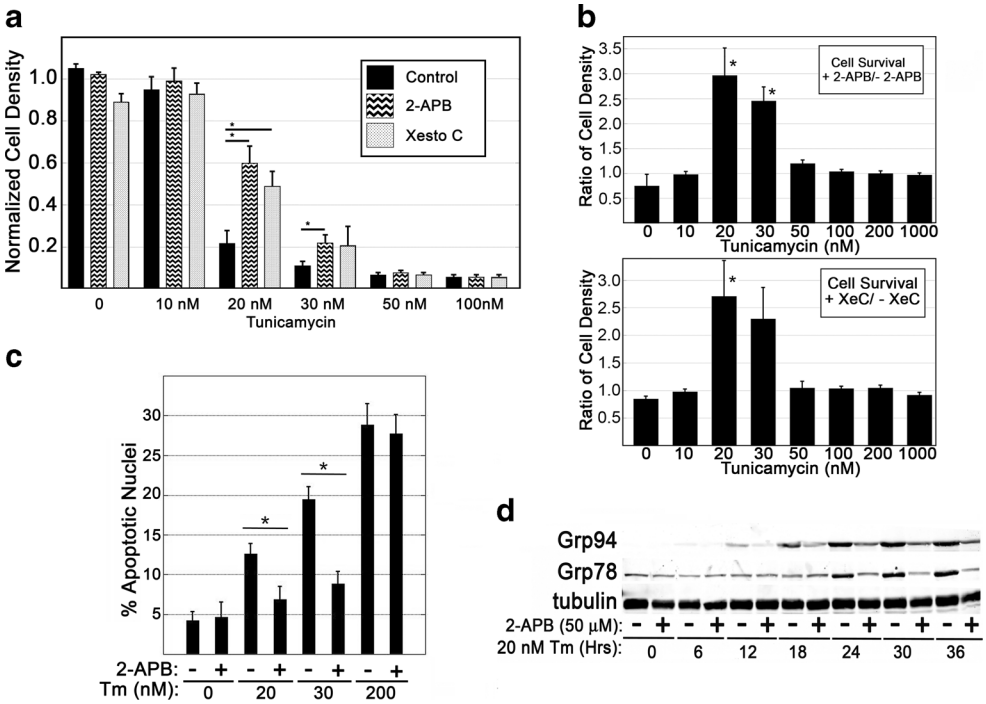

Fig. 3 ER stress-induced apoptosis in BHK21 cells is susceptible to ITPR inhibition only at moderate doses of Tm. **a**, **b** BHK21 cells were seeded at a density of 15,000 cells/cm^2, exposed to varied doses of Tm for 48 h, and assessed for density of adherent cells via crystal violet staining. The density ratio of cells cultured in the presence or absence of ITPR-inhibitor (2-APB, 50 μM, or Xestospongin C, 10 μM) was determined. **c** Cells were treated with Tm doses in the presence or absence of ITPR inhibitor for a period of 36 h. Apoptotic nuclear morphology was quantified via nuclear staining (DAPI) and assessment via fluorescence microscopy. **d** Immunoblot analysis of UPR responses at moderate dosage of Tm in the presence or absence of ITPR inhibitor. Blots shown are representative of at least three independently replicated experiments. Statistical analysis was via Student's *t* test comparing individual Tm doses to matched doses with ITPR inhibitor ($p < 0.05$)

44) and p38 activation were performed. Cells were exposed to doses of Tm ranging from 20 to 1000 nM for a period of 8 h (Fig. 5a, b). Immunoblot analysis revealed Erk1/2 activation to be limited to moderate doses of Tm, while p38 activation increased with dosage of Tm exposure. Inhibitor of apoptosis (IAP) proteins, survivin and cIAP1, were assessed for their response to varying doses of Tm. IAP family members have been shown to inhibit caspase activity, and diminished IAP protein presence in the cytosol is one characteristic of apoptosis activation. Survivin displayed a more rapid decrease following ER stress, though decreases of both proteins correlated with Tm dose and intensified over time (Fig. 5c).

Profiles of cell density during Tm exposure were performed in the presence or absence of inhibitors of ER stress signaling (IRE1, PERK) and well-known cytosolic stress signaling mediators (p38, Jnk1, and Erk1/2). Cells were stressed with varied concentrations of Tm, and cell density assessed after 48 h. At moderate doses of Tm up to 50 nM, PERK

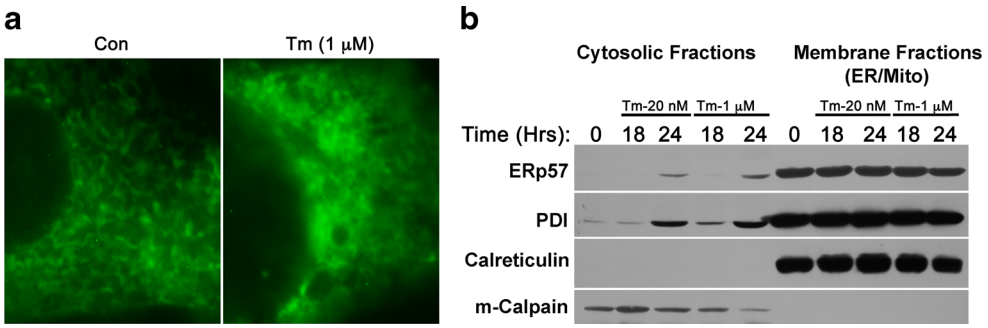

Fig. 4 Moderate and severe ER stress similarly impact ER membrane integrity. **a** BHK21 cells were transfected with a plasmid encoding an ER-restricted GFP (pGFP-ER) and subsequently assessed for distribution of green fluorescence under control and ER stress conditions. **b** Cells were exposed to moderate (20 nM) and high (200 nM) doses of Tm for indicated time points and then assessed for distribution of proteins normally associated with the ER lumen (ERp57, PDI, calreticulin). m-Calpain was assessed as a control for cytosolic components. Both moderate and severe ER stress generated release of ERp57 and PDI from the ER lumen to the cytosol. Blots are representative of two replicated experiments

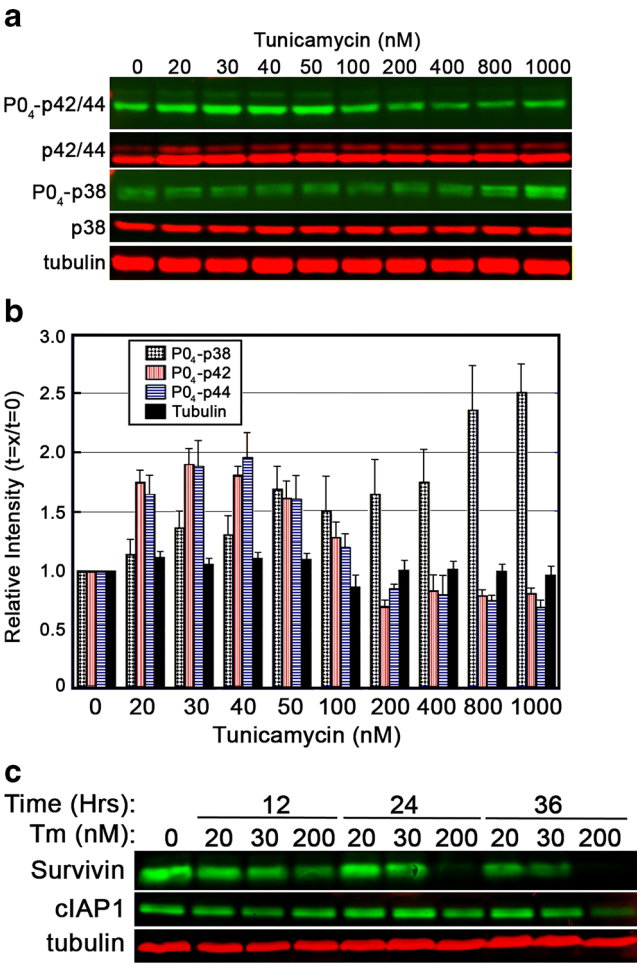

Fig. 5 Dosage of Tm differentially influences the Erk1/2 and p38 signaling pathways. **a**, **b** BHK21 cells were exposed to varied doses of Tm for a period of 8 h and then assessed for activation of the Erk1/2 (p42/p44) and p38 signaling pathways. Relative intensity of activation was determined by normalizing bands to the vehicle-treated control. Erk1/2 show elevated phosphorylation (activation) over moderate doses of Tm, and activation of the p38 stress-activated protein kinase increased with Tm dose. **c** Anti-apoptotic regulatory proteins survivin and cIAP1 decrease in BHK21 cells with increasing loss associated with higher doses of Tm. All blots shown are representative of at least three replicated experiments

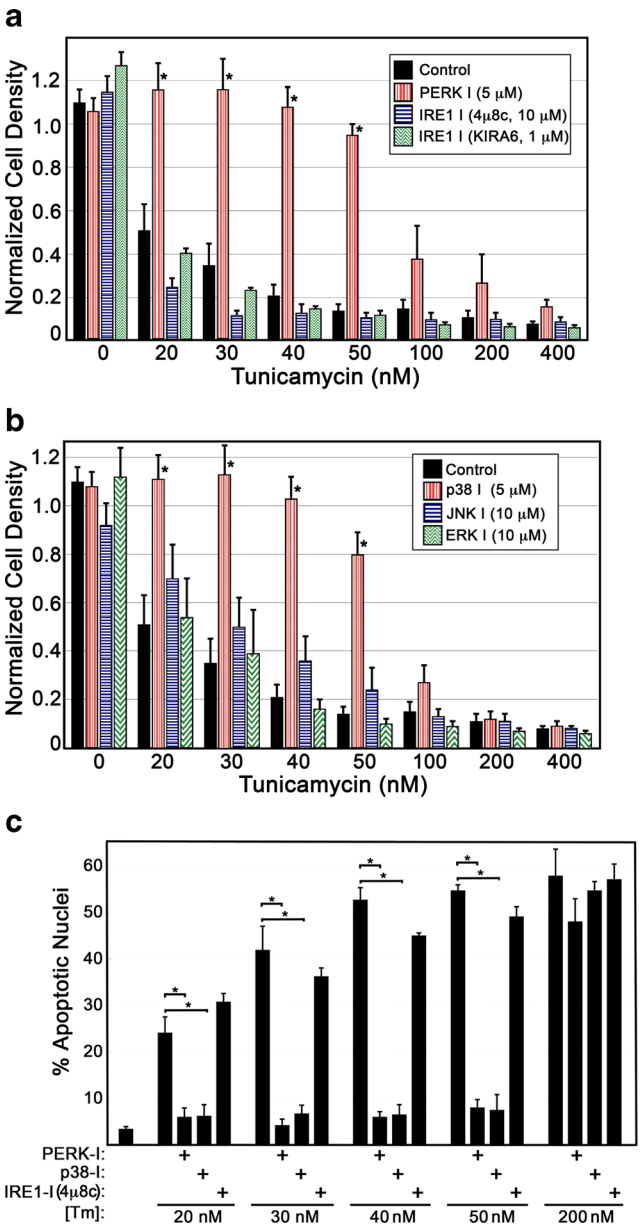

Fig. 6 Inhibition of p38 or PERK is sufficient to arrest apoptosis in cells experiencing moderate ER stress. **a** BHK21 cells were exposed to varying doses of Tm in the presence or absence of inhibitors of IRE1 or PERK (48-h exposure). Inhibition of PERK was sufficient to arrest decreases in cell density at Tm doses up to 50 nM, while inhibition of IRE1 displayed no discernable impact. **b** Cells were exposed to varying doses of Tm in the presence or absence of inhibitors of the p38 or JNK1 stress-activated kinases or the Erk1/2 kinases. Inhibition of p38 activity was sufficient to protect cells from decreases in cell density at Tm doses up to 50 nM, while the other inhibitors had no detectable affect. **c** Analysis of nuclear morphology was performed via DAPI staining of fixed cells and fluorescence microscopy to quantify frequency of apoptotic cells. Inhibition of either PERK or p38 protected cells from activation of apoptosis at Tm doses of 20–50 nM (36-h exposure). For **a**–**c**, statistical analysis was by ANOVA with a Tukey's all pairs post hoc test comparing all samples at each dose of Tm ($p < 0.05$)

inhibition was sufficient to significantly diminish Tm-induced decreases in cell density (Fig. 6a). Inhibition of IRE1 activation by blocking oligomerization (4u8c) or blocking kinase activity (KIRA6) did not display significant levels of protection in this assay. Though Erk1/2 activity was shown to be elevated at moderate doses of ER stress (Fig. 5b), inhibition of these kinases had no affect on Tm-induced changes in cell density (Fig. 6b). Inhibition of p38 kinase activity displayed a pattern of protection similar to PERK inhibition, blocking Tm-induced decreases in cell density at moderate doses of Tm exposure up to 50 nM. Analysis of apoptotic nuclei revealed inhibition of PERK or p38, but not IRE1, to inhibit apoptotic activation at moderate doses of Tm (Fig. 6c). It should be noted that higher doses of inhibitors were evaluated and showed no additional capacity to protect cells from ER stress-induced apoptosis. In the case of KIRA6 and PERK

inhibitor 1, higher doses than those shown were toxic, generating significant cell loss in control wells.

PERK activation results in the suppression of general cellular translation via phosphorylation of eIF2α, which arrests the translation of most cellular transcripts. This decrease in the production of many proteins may contribute to the decline of anti-apoptotic proteins shown previously (Fig. 5c). Salubrinal was used to examine if eIF2α phosphorylation alone was sufficient to generate a decrease in anti-apoptotic Mcl-1 and survivin protein levels. Inhibition of the Gadd34 eIF2α phosphatase with salubrinal results in a gradual accumulation of eIF2a phosphorylation on serine 51 (Fig. 7a/b). Over a 36-h treatment, salubrinal alone was sufficient to generate a significant reduction in both Mcl-1 and survivin (Fig. 7c). Inclusion of the MG132 proteasome inhibitor completely blocked this affect, revealing protein degradation to play a central role in the loss of these proteins.

To evaluate the impact of PERK inhibition upon stress signaling induced by moderate and severe ER stress, panels of immunoblots were performed. ER stress was shown to activate a PERK-dependent phosphorylation of eIF2a and elevation of both ATF4 and CHOP protein levels. In addition, moderate doses of Tm generated a PERK-dependent phosphorylation of p38 and decreases in anti-apoptotic Mcl-1 and survivin protein levels (Fig. 7d). As is summarized in Fig. 7e, this data is supportive of a model that presents PERK as a key regulator of apoptotic signaling in cells experiencing moderate levels of ER stress.

Discussion

Endoplasmic reticulum stress generates a complex array of cellular signals, inducing changes in gene expression, cellular

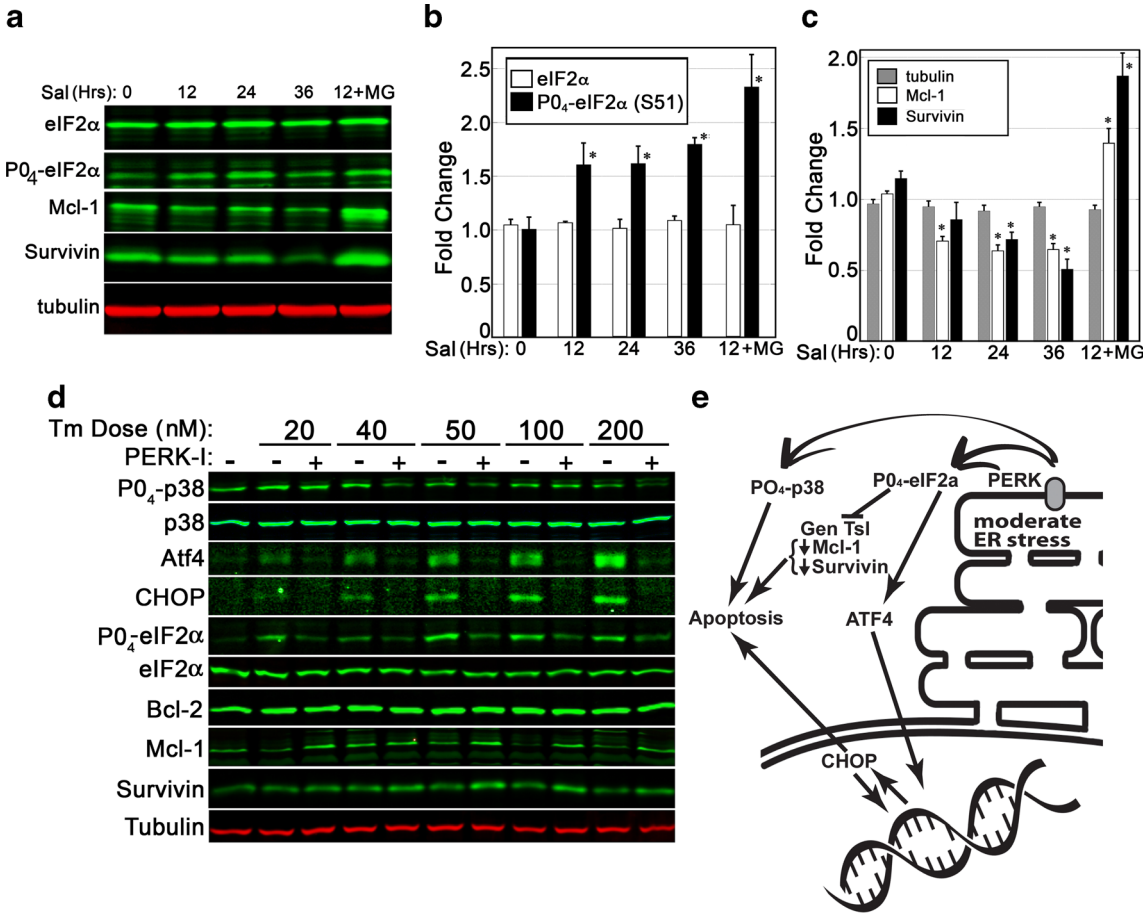

Fig. 7 PERK activity plays a central role in pro-apoptotic cellular changes during ER stress. **a**–**c** A 36-h time course of salubrinal exposure (10 μM) was used to assess if eIF2α phosphorylation was sufficient to cause a decline in anti-apoptotic proteins. Quantitative analysis of BHK21 cell lysates revealed salubrinal, an inhibitor of the Gadd34 phosphatase, to cause a significant accumulation of phosphorylated eIF2α within 12 h. Levels of Mcl-1 and survivin proteins declined gradually over time. Inclusion of a proteasome inhibitor (MG132, 5 mM) was sufficient to arrest the decline in Mcl-1 and survivin. **d** BHK21 cells were exposed to varying doses of Tm over a period of 24 h and then analyzed via immunoblot. Inhibition of PERK was sufficient to suppress phosphorylation of p38 and eIF2α, decreases in survivin and Mcl-1, and induced expression of ATF4 and CHOP. Blots shown are representative of two replicated experiments. **e** A summary of PERK impacts upon stress signaling and apoptosis. Statistical assessment for b/c was by ANOVA with a Tukey's all pairs post hoc text comparing samples at each time point to control ($p < 0.5$)

biochemistry, and signaling networks. This study originated from a simple observation that the intensity of ER stress exposure generates unique apoptotic signaling, revealing this stress exposure to generate diverse responses depending upon stress intensity. This was initially revealed by differences in apoptotic signaling in tsBN7 cells displaying temperature-induced or toxin-induced defects in N-linked glycosylation. The dosage of Tm used in this initial analysis was consistent with that commonly used in ER stress signaling studies. IRE1 splicing activity and PERK activation are readily quantifiable measures of ER stress signaling whose activity varies in a dose/response relationship with Tm dose. As hypothesized, differences between the TS and Tm treatments were revealed in the magnitude of IRE1 splicing activity and PERK-dependent eIF2α phosphorylation. A titration of Tm concentrations revealed doses of approximately 20–40 nM to mimic the level of ER stress signaling induced by TS conditions. Moderate doses of Tm generated apoptotic signaling in parental BHK21 cells that was susceptible to ITPR inhibition in a manner similar to TS-treated tsBN7 cells. This dosage-dependent difference in signaling reveals an important consideration for studies evaluating ER stress or employing ER stress as an activator of specific physiological responses.

A previous study by Rutkowski et al. examined mild ER stress by using mouse embryonic fibroblast (MEF) cell lines (Rutkowski et al. 2006). They found that moderate doses of Tm or thapsigargin (Tg) transiently activated all three central ER stress sensors: IRE1, PERK, and ATF6. Examination of ER morphology with electron microscopy revealed both moderate and higher doses of Tm to generate dilation of the organelle, fragmentation, and evidence of protein aggregates (Rutkowski et al. 2006). These MEFs displayed a capacity for long-term survival and even moderate growth in the presence of Tm at 25 ng/ml (30 nM). These stress-adapted MEF cells displayed higher rates of mRNA decay for transcripts encoding proteins with pro-apoptotic influence (CHOP, ATF4, Gadd34). In comparison, we found that BHK21 cells display apoptosis at 20 nM Tm or higher and a clear induction of both PERK and IRE1 signaling. When comparing moderate and high doses of Tm in BHK21 cells (20 and 200 nM), cell fractionation studies showed similar affects upon ER membrane integrity. These observations of changes in ER morphology and integrity at moderate levels of ER stress raise interesting questions regarding the potential reversal of this process and ER adaptation during chronic stress.

Analysis of cellular signaling behavior revealed the p38 stress-activated protein kinase to be induced in a manner that correlates with Tm dose. In contrast, the Erk1/2 (p42/44) kinases were induced only at moderate doses of Tm, with peak activation being observed at 20–50 nM. Erk1/2 signaling has been associated with ER stress in prior studies and in some cases has been shown to serve a pro-survival or autophagy-inducing role in the cellular response (Arai et al. 2004; Jiang et al. 2007; Ghosh et al. 2015). Inhibition of the MEK/ERK pathway was recently shown to dramatically increase apoptosis activation in breast cancer cells experiencing ER stress (Ghosh et al. 2015). The restriction of Erk1/2 signaling to lower doses of Tm in our study may identify an important protective measure induced by cells during adaptation to survivable levels of ER dysfunction. We note that ERK inhibition did not clearly exacerbate apoptosis activation in our analysis, though the observation of elevated activity merits additional evaluation. Two IAP family members, cIAP1 (BIRC2) and survivin (BIRC5), displayed a clear susceptibility to ER stress in a dosage-dependent manner. In addition, two mitochondrial membrane proteins that play a predominantly inhibitory role in apoptotic activation were assessed. Bcl-2 protein and induced myeloid leukemia cell differentiation protein (Mcl-1) each are predominantly located in the outer mitochondrial membrane and suppress activation of the mitochondrial permeability transition to induce apoptosis (Czabotar et al. 2014; Opferman 2015). During ER stress, Mcl-1 but not Bcl-2 declined in a Tm dose-dependent manner (Fig. 7d). These results correlate with higher levels of apoptosis observed at higher doses of Tm. The loss of these proteins is PERK-dependent and likely due to increased phosphorylation of eIF2α and arrest of generalized translation. Indeed, inducing eIF2α phosphorylation in the absence of ER stress was sufficient to cause a loss of Mcl-1 and survivin (Fig. 7a–c). Conversely, inhibition of PERK kinase activity during ER stress was shown to arrest the loss of these proteins (Fig. 7d). One published report noted ER stress to moderately induce expression of some IAP family members in a PERK-dependent manner (Hamanaka et al. 2009). Our results are in contrast with their result both in defining PERK activity as purely protective and in PERK activity facilitating an increase in IAP expression. A decline in IAP members following ER stress has been noted in other studies as well (Hiramatsu et al. 2014; Sohn et al. 2003; Lim et al. 2015), though our study links PERK activity to induce this decline. The observed PERK-induced declines in anti-apoptotic proteins during ER stress reveal key changes in cellular posture in relation to apoptosis activation.

The central finding defined in this manuscript reveals apoptosis activation, during moderate levels of ER stress, to be stimulated through PERK and the p38 stress-activated protein kinase. Inhibition of PERK diminished ER stress-induced phosphorylation of p38, consistent with this cytosolic signal being downstream of PERK activity. PERK has been shown to activate apoptosis through p38 in studies of selenite-induced apoptosis in leukemia cells (Jiang et al. 2014). This work revealed PERK to activate p38 by destabilizing the association of p38 with a cytosolic Cdc37/Hsp90 protein complex. Though p38 activation via several kinase pathways is well known, non-canonical activation via autophosphorylation has also been observed (Ashwell 2006; Kim et al. 2005). Fungal orthologs of p38 (Hog1) contain a C-terminal

domain element that suppresses this autophosphorylation mechanism. In mammalian cells, inhibition of this autophosphorylation is mediated via formation of the p38/Cdc37/Hsp90 complex in the cellular cytosol (Ota et al. 2010). Pharmacological inhibition of Hsp90 is sufficient to activate p38 release from this complex followed by autophosphorylation at Thr^{180} and Tyr^{182} (TGY activation motif) and activation of apoptosis (Manni et al. 2012). Direct interaction of active PERK with Hsp90 has been observed via immunoprecipitation and colocalization studies, though the mechanism for inducing p38 release is unknown (Jiang et al. 2014). The role of p38 in activating apoptosis during ER stress seems to focus upon the cellular decision between autophagy and apoptosis. As levels of the ATF4 transcription factor increase following eIF2α phosphorylation, this protein has the ability to induce pro-autophagy and pro-apoptosis genes. In the presence of active p38, ATF4 binding favors pro-apoptosis targets, such as CHOP (Jiang et al. 2014; Liu et al. 2015). Our data support a model that includes PERK activation of p38 to induce apoptosis during moderate ER stress (Fig. 7e). At higher doses of ER stress, inhibition of these components is insufficient to arrest apoptotic progress, indicating that additional signaling mechanisms are involved.

Conclusions

This manuscript explores distinct patterns of signaling exhibited by varied doses of ER stress. Defects in N-linked glycosylation activate ER stress signaling that is responsive to the severity of the deficiency. A titration of Tm doses revealed moderate deficiency but not severe deficiency of N-linked glycosylation to elevate levels of Erk1/2 phosphorylation, while p38 phosphorylation increased with Tm dose. Moderate ER stress exhibited apoptotic influences upon the cell via signaling from the ER transmembrane PERK protein and a subsequent activation of the p38 stress-activated protein kinase. Arrest of general cellular translation via PERK-mediated phosphorylation of eIF2α was sufficient to cause a gradual decline in the levels of anti-apoptotic proteins that include Mcl-1 and survivin. These results are consistent with studies linking PERK activity to activation of p38 via destabilization of an inhibitory p38/Cdc37/Hsp90 protein complex. This study reveals the severity of ER stress to modulate signaling behaviors, with the ER acting as a rheostat of stress signaling rather than an on/off switch.

Acknowledgments The authors wish to recognize the helpful contributions of research students Celina Jones, Emily Blair, and Tina Johnson. This work was supported by grants from the National Institutes of Health (R15GM065139), the National Science Foundation (DBI-1062721), and research funding from Pepperdine University.

References

Arai K et al (2004) Involvement of ERK MAP kinase in endoplasmic reticulum stress in SH-SY5Y human neuroblastoma cells. J Neurochem 89(1):232–239

Ascher-Landsberg J et al (1999) The effects of 2-aminoethoxydiphenyl borate, a novel inositol 1,4, 5-trisphosphate receptor modulator on myometrial contractions. Biochem Biophys Res Commun 264(3): 979–982

Ashwell JD (2006) The many paths to p38 mitogen-activated protein kinase activation in the immune system. Nat Rev Immunol 6(7): 532–540

Blackshaw S et al (2000) Type 3 inositol 1,4,5-trisphosphate receptor modulates cell death. FASEB J 14(10):1375–1379

Boehning D et al (2003) Cytochrome c binds to inositol (1,4,5) trisphosphate receptors, amplifying calcium-dependent apoptosis. Nat Cell Biol 5(12):1051–1061

Boyce M et al (2005) A selective inhibitor of eIF2alpha dephosphorylation protects cells from ER stress. Science 307(5711):935–939

Brewster JL et al (2000) Deletion of Dad1 in mice induces an apoptosis-associated embryonic lethality. Genesis 26:271–278

Cnop M et al (2007) Selective inhibition of eukaryotic translation initiation factor 2 alpha dephosphorylation potentiates fatty acid-induced endoplasmic reticulum stress and causes pancreatic beta-cell dysfunction and apoptosis. J Biol Chem 282(6):3989–3997

Czabotar PE et al (2014) Control of apoptosis by the BCL-2 protein family: implications for physiology and therapy. Nat Rev Mol Cell Biol 15(1):49–63

Gardner BM, Walter P (2011) Unfolded proteins are Ire1-activating ligands that directly induce the unfolded protein response. Science 333(6051):1891–1894

Gardner BM et al (2013) Endoplasmic reticulum stress sensing in the unfolded protein response. Cold Spring Harb Perspect Biol 5(3): a013169

Ghosh S et al (2015) Cross-talk between endoplasmic reticulum (ER) stress and the MEK/ERK pathway potentiates apoptosis in human triple negative breast carcinoma cells: role of a dihydropyrimidone, nifetepimine. J Biol Chem 290(7):3936–3949

Hamanaka RB et al (2009) PERK-dependent regulation of IAP translation during ER stress. Oncogene 28(6):910–920

Hassler J, Cao SS, Kaufman RJ (2012) IRE1, a double-edged sword in pre-miRNA slicing and cell death. Dev Cell 23(5):921–923

Hetz C (2012) The unfolded protein response: controlling cell fate decisions under ER stress and beyond. Nat Rev Mol Cell Biol 13(2):89–102

Higo T et al (2010) Mechanism of ER stress-induced brain damage by IP(3) receptor. Neuron 68(5):865–878

Hiramatsu N et al (2014) Translational and posttranslational regulation of XIAP by eIF2alpha and ATF4 promotes ER stress-induced cell death during the unfolded protein response. Mol Biol Cell 25(9): 1411–1420

Hiramatsu N et al (2015) Multiple mechanisms of unfolded protein response-induced cell death. Am J Pathol 185:1800–1808

Hong NA et al (2000) Mice lacking Dad1, the defender against apoptotic death-1, express abnormal N-linked glycoproteins and undergo increased embryonic apoptosis. Dev Biol 220(1):76–84

Hoppins S, Nunnari J (2012) Cell biology. Mitochondrial dynamics and apoptosis—the ER connection. Science 337(6098):1052–1054

Jiang CC et al (2007) Inhibition of MEK sensitizes human melanoma cells to endoplasmic reticulum stress-induced apoptosis. Cancer Res 67(20):9750–9761

Jiang Q et al (2014) Involvement of p38 in signal switching from autophagy to apoptosis via the PERK/eIF2alpha/ATF4 axis in selenite-treated NB4 cells. Cell Death Dis 5:e1270

Joseph SK, Hajnoczky G (2007) IP3 receptors in cell survival and apoptosis: Ca2+ release and beyond. Apoptosis 12(5):951–968

Kessel D (2006) Protection of Bcl-2 by salubrinal. Biochem Biophys Res Commun 346(4):1320–1323

Kim L et al (2005) p38 MAPK autophosphorylation drives macrophage IL-12 production during intracellular infection. J Immunol 174(7): 4178–4184

Lee AS (2005) The ER chaperone and signaling regulator GRP78/BiP as a monitor of endoplasmic reticulum stress. Methods 35(4):373–381

Lim EJ, Heo J, Kim YH (2015) Tunicamycin promotes apoptosis in leukemia cells through ROS generation and downregulation of survivin expression. Apoptosis 20(8):1087–1098

Liu Z et al (2015) Protein kinase R-like ER kinase and its role in endoplasmic reticulum stress-decided cell fate. Cell Death Dis 6:e1822

Manni S et al (2012) Protein kinase CK2 protects multiple myeloma cells from ER stress-induced apoptosis and from the cytotoxic effect of HSP90 inhibition through regulation of the unfolded protein response. Clin Cancer Res 18(7):1888–1900

Maurel M et al (2014) Getting RIDD of RNA: IRE1 in cell fate regulation. Trends Biochem Sci 39(5):245–254

Miyamoto S et al (2000) Xestospongin C, a selective and membrane-permeable inhibitor of IP(3) receptor, attenuates the positive inotropic effect of alpha-adrenergic stimulation in Guinea-pig papillary muscle. Br J Pharmacol 130(3):650–654

Nakashima T et al (1993) Molecular cloning of a human cDNA encoding a novel protein, DAD1, whose defect causes apoptotic cell death in hamster BHK21 cells. Mol Cell Biol 13(10):6367–6374

Niederer KE et al (2005) Cypermethrin blocks a mitochondria-dependent apoptotic signal initiated by deficient N-linked glycosylation within the endoplasmic reticulum. Cell Signal 17:177–186

Nikonov AV et al (2002) Active translocon complexes labeled with GFP-Dad1 diffuse slowly as large polysome arrays in the endoplasmic reticulum. J Cell Biol 158(3):497–506

Opferman JT (2015) Attacking cancer's Achilles heel: antagonism of anti-apoptotic BCL-2 family members. FEBS J. doi:10.1111/febs.13472

Ota A et al (2010) Specific regulation of noncanonical p38alpha activation by Hsp90-Cdc37 chaperone complex in cardiomyocyte. Circ Res 106(8):1404–1412

Ruggiano A, Foresti O, Carvalho P (2014) Quality control: ER-associated degradation: protein quality control and beyond. J Cell Biol 204(6): 869–879

Rutkowski DT et al (2006) Adaptation to ER stress is mediated by differential stabilities of pro-survival and pro-apoptotic mRNAs and proteins. PLoS Biol 4(11):e374

Saleem H et al (2014) Interactions of antagonists with subtypes of inositol 1,4,5-trisphosphate (IP3) receptor. Br J Pharmacol 171(13):3298–3312

Sanjay A, Fu J, Kreibich G (1998) DAD1 is required for the function and the structural integrity of the oligosaccharyltransferase complex. J Biol Chem 273(40):26094–26099

Schroder M (2008) Endoplasmic reticulum stress responses. Cell Mol Life Sci 65(6):862–894

Sohn J et al (2003) The effect of ursodeoxycholic acid on the survivin in thapsigargin-induced apoptosis. Cancer Lett 191(1):83–92

Upton JP et al (2012) IRE1alpha cleaves select microRNAs during ER stress to derepress translation of proapoptotic caspase-2. Science 338(6108):818–822

Walter P, Ron D (2011) The unfolded protein response: from stress pathway to homeostatic regulation. Science 334(6059):1081–1086

Wang X et al (2011) Bcl-2 proteins regulate ER membrane permeability to luminal proteins during ER stress-induced apoptosis. Cell Death Differ 18(1):38–47

Wek RC, Jiang HY, Anthony TG (2006) Coping with stress: eIF2 kinases and translational control. Biochem Soc Trans 34(Pt 1):7–11

Wu L et al (2014) Salubrinal protects against rotenone-induced SH-SY5Y cell death via ATF4-parkin pathway. Brain Res 1549:52–62

Zhu X et al (2014) Ubiquitination of inositol-requiring enzyme 1 (IRE1) by the E3 ligase CHIP mediates the IRE1/TRAF2/JNK pathway. J Biol Chem 289(44):30567–30577

Zong WX et al (2003) Bax and Bak can localize to the endoplasmic reticulum to initiate apoptosis. J Cell Biol 162(1):59–69